PHILOSOPHICAL TRANSACTIONS OF THE ROYAL SOCIETY A MATHEMATICAL, PHYSICAL & ENGINEERING SCIENCES

Chemical Vapour Deposition of Diamond

John C. Angus, Alberto Argoitia, Roy Gat, Zhidan Li, Mahendra Sunkara, Long Wang and Yaxin Wang

Phil. Trans. R. Soc. Lond. A 1993 **342**, 195-208
doi: 10.1098/rsta.1993.0014

Chemical vapour deposition of diamond

By John C. Angus, Alberto Argoitia, Roy Gat, Zhidan Li, Mahendra Sunkara, Long Wang and Yaxin Wang

Department of Chemical Engineering, Case Western Reserve University, Cleveland, Ohio 44106, U.S.A.

Growth of diamond at conditions where it is the metastable phase can be achieved by various chemical vapour deposition methods. Atomic hydrogen plays a major role in mediating rates and in maintaining a proper surface for growth. Low molecular weight hydrocarbon species (e.g. CH_3 and C_2H_x) are believed to be responsible for extension of the diamond lattice, but complete understanding of attachment mechanisms has not yet been achieved. The nucleation of diamond crystals directly from the gas phase can proceed through a graphitic intermediate. Once formed, the growth rate of diamond crystals is enhanced by the influence of stacking errors. Many of the commonly observed morphologies, e.g. hexagonal platelets and (apparent) decahedral and icosahedral crystals, can be explained by the influence of simple stacking errors on growth rates. *In situ* measurements of growth rates as a function of hydrocarbon concentration show that the mechanism for diamond growth is complex and may involve surface adsorption processes in rate limiting steps. The transport régime in diamond deposition reactors varies widely. In the hot-filament and microwave reactors, which operate from 20 to 100 Torr (1 Torr $\approx$ 133 Pa), the transport of mass and energy is dominated by molecular diffusion. In the atmospheric pressure combustion and plasma methods, transport is dominated by convection. *In situ* measurements of H atom recombination rates in hot-filament reactors show that, under many commonly used process conditions, transport of atomic hydrogen to the growing surface is diffusion limited and H atom recombination is a major contributor to energy transport.

1. Introduction

Diamond synthesis by chemical vapour deposition (CVD), at pressures and temperatures where diamond is metastable with respect to graphite, was first achieved by William G. Eversole of the Union Carbide Corporation (Eversole 1962). Unpublished reports show that Eversole achieved growth of new diamond during the period 26 November 1952 to 7 January 1953 (A. D. Kiffer). This is just before 15 February 1953, the date of the first high-pressure–high-temperature synthesis of diamond by Liander & Lundblad (1960) at Allemana Svenska Eliktriska Aktiebolaget (ASEA), and well ahead of the synthesis by General Electric in 1954.

Efforts to grow diamond at low pressures arose independently of each other and without knowledge of the Eversole work in both the Soviet Union and the United States (Spitsyn & Deryagin 1956; Angus 1961). The first published papers from these groups did not appear until much later (Angus *et al.* 1968; Deryagin *et al.* 1968). The use of atomic hydrogen to etch graphitic deposits (Angus *et al.* 1971) and its use during growth to permit high rate nucleation and growth of diamond on non-

Phil. Trans. R. Soc. Lond. A (1993) **342**, 195–208
Printed in Great Britain

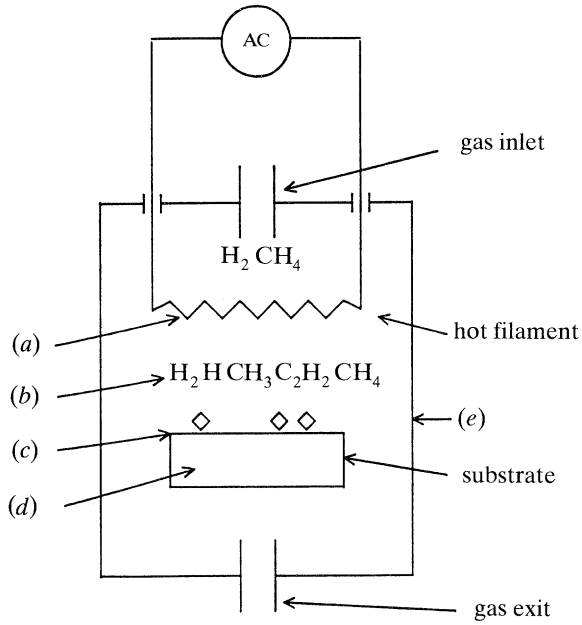

Figure 1. Schematic diagram of hot-filament chemical vapour deposition reactor (permission of *A. Rev. Mater. Sci.*). Reaction numbers refer to table 1. (*a*) Reaction 1; (*b*) gas phase reactions 2–6; (*c*) surface reactions 7–9; (*d*) solid state diffusion, carbide formation; (*e*) wall reactions.

diamond substrates (Deryagin *et al.* 1976) followed. The current intense level of interest can be traced to the Japanese group at the National Institute for Research in Inorganic Materials (NIRIM) in Tsukuba, Japan. They revealed details of several methods for the CVD of diamond, including the widely used hot-filament and microwave plasma assisted techniques (Matsumoto *et al.* 1982*a*, *b*; Kamo *et al.* 1983; Matsui *et al.* 1983).

Details of the history of diamond synthesis have been extensively reported elsewhere and will not be repeated here (Davies 1984; DeVries 1987; Badzian & DeVries 1988; Angus 1989, 1990).

Diamond has long been known to be thermodynamically stable with respect to graphite only at high pressure (Leipunski 1939; Berman & Simon 1955). This fact was erroneously interpreted by many workers to mean that diamond could never be synthesized at low pressures, where graphite is the stable form of carbon. A notable exception to this view was Bridgman (1955).

Diamond is, in fact, only slightly unstable with respect to graphite. At 298 K and 1 atm† pressure, the difference in free energy between diamond and graphite is only 2.900 kJ mol^{-1} (approximately 0.03 eV per atom), which is only on the order of kT. Furthermore, there is a very large activation barrier inhibiting the transformation of diamond to graphite. Of perhaps more significance is the fact that graphite (2.26 g cm^{-3}) is less dense than diamond (3.51 g cm^{-3}). Therefore as solid carbon precipitates out of a supersaturated carbon gas, the 'first' phase encountered is graphite, not diamond. This is an example of Volmer's rule, which states that the least dense solid phase is the first to crystallize from a supersaturated fluid phase. Once formed, graphite will not spontaneously transform further into diamond

† 1 atm $\approx 10^5$ Pa.

because it is the stable phase and because of the high activation barrier between the two phases. However, atomic hydrogen changes the relative energies of small graphitic and diamond nuclei and provides a means for circumventing the large activation barrier. This will be discussed in more detail in §3 below.

In CVD of diamond from C/H and C/H/O gas mixtures the gas phase is decomposed to atomic hydrogen, molecular fragments, free radicals and sometimes ions. The most commonly used methods are various types of plasma discharges, heated filaments and combustion. Diamond is formed from these complex gas phase reaction mixtures on substrates held at nominal temperatures from 700 °C to 1000 °C. A simple schematic of a hot-filament reactor is shown in figure 1. Although details of the complex reaction and transport processes are still the subject of much research, a general understanding of the reactor environment and the principal reactions and energy flows has been achieved.

2. Diamond growth

Some of the principal reactions of importance are summarized in table 1 with an estimate of their standard enthalpy and free energy changes. Examination of table 1 gives a clear picture of the basic energetics of the entire diamond deposition process. The principal function of the hot filament, or equivalently the plasma discharge, is to provide large amounts of atomic hydrogen through the decomposition of molecular hydrogen (reaction 1). This reaction has a very positive enthalpy change.

The atomic hydrogen, once formed, undergoes several spontaneous, highly exothermic, reactions. It can react with hydrocarbons in the gas phase, abstracting hydrogen to form methyl radicals (reaction 2). Recombination of atomic hydrogen to form molecular hydrogen (reaction 3) is also possible. However, since this is a three body reaction, its rate is slow at low reactor pressures and often can be ignored despite the favourable free energy change. Methyl radical destruction can take place by recombination with atomic hydrogen (reaction 4) or by diffusion out of the reaction zone to the walls of the reactor. There are gas phase reaction paths to higher molecular weight species, e.g. reaction 5. A spectrum of C_2H_x species can be formed by subsequent hydrogen atom abstraction reactions of the general type shown in reaction 6. These can lead to still higher molecular weight compounds by subsequent reactions not shown in table 1.

Atomic hydrogen will hydrogenate a bare diamond surface (reaction 7). Hydrogenated diamond surfaces are less prone to surface reconstruction than bare surfaces. On (111) surfaces, for example, bonded hydrogen helps maintain the bulk terminated diamond surface structure (Lander & Morrison 1964). Hydrogen can also abstract hydrogen from a hydrogen covered surface (reaction 8). This reaction is thermodynamically favoured because of the strong H–H bond. At typical substrate temperatures the fractional coverage is dominated by the competition between reactions 7 and 8. To first order, the steady state concentration of free radical sites, f_s, is independent of the atomic hydrogen concentration and is approximately given by the competition between reactions 7 and 8

$$f_s = k_8/(k_7 + k_8), \tag{1}$$

where k_7 and k_8 are the first order rate constants for reactions 7 and 8. f_s can be estimated using kinetic constants for analogous gas phase reactions. At temperatures

PHILOSOPHICAL TRANSACTIONS OF THE ROYAL SOCIETY A MATHEMATICAL, PHYSICAL & ENGINEERING SCIENCES

Table 1. *Standard enthalpy and free energy changes of some important reactions during diamond growth*

(1 kcal = 4.184 kJ.)

	reaction	T/K	ΔH^0/(kcal mol^{-1})	ΔG^0/(kcal mol^{-1})[a]
	on filament			
1	$H_2 \rightarrow 2H$	2500	+109	+37[b]
	in gas phase			
2	$H + CH_4 \rightarrow CH_3 + H_2$	1800	*ca.* 0	−11
3	$H + H + M \rightarrow H_2 + M$	1800	−108	−57
4	$CH_3 + H + M \rightarrow CH_4 + M$	1800	−108	−45
5	$CH_3 + CH_3 + M \rightarrow C_2H_6 + M$	1800	−86[c]	−26[c]
6	$C_2H_x + H \rightarrow C_2H_{x-1} + H_2$	1800	small	small
	on substrate (S)			
7	$H + S \rightarrow S\text{–}H$	1200	−94	−68
8	$S\text{–}H + H \rightarrow S + H_2$	1200	−13	−6
9	$CH_3 + S \rightarrow S\text{–}CH_3$	1200	−81	−47

[a] Rossini & Jessup (1938), Stull *et al.* (1969) and Stull & Prophet (1971).
[b] At 20 Torr and 2500 K, the equilibrium mole fraction of atomic H is 0.16.
[c] Molecular mechanics estimate.

of 1000 and 1750 K, f_s was estimated to be 0.12 and 0.37 respectively (Kuczmarski 1992). These sites are where free radicals such as CH_3 (reaction 9) or acetylenic species, C_2H_x, can add to the surface. Finally, the H atom recombination on the surface contributes substantially to the energy flux delivered to the substrate. The recombination could be direct through reaction 3 where the surface plays the role of the third body or it could result as the net reaction from the two step process of reactions 7 and 8.

Much attention has focused on identification of the gas phase 'growth species' that are responsible for the addition of carbon to the diamond surface. Methyl radical, CH_3, and acetylene, C_2H_2, are believed to be the most likely candidates. Recent evidence, for example the isotope labelling studies of Chu *et al.* (1991) indicate that the methyl radical is the primary source of added carbon. The state of understanding has been the subject of an excellent recent review by Celii & Butler (1991) in which they summarized the extensive studies of Tsuda, Frenklach, Harris, Hauge and others. A recent molecular dynamics study by Garrison *et al.* (1992) of growth on the diamond (001) surface is also of great interest.

Recent microbalance studies of diamond growth kinetics show a complex behaviour. In a hot-filament reactor at 20 Torr†, the growth rate of diamond was first order in methane from 0.1% to 1.0% CH_4 (Wang *et al.* 1992). At high methane concentrations, the reaction tended to zero order. For the two-carbon source gases, C_2H_2, C_2H_4 and C_2H_6, the reaction was approximately one half order for concentrations from 0.3% to 1.0% hydrocarbon. Below a concentration of 0.3% hydrocarbon, the two-carbon gases showed a first order rate (see figure 2). The data are in agreement with a much earlier study (Chauhan *et al.* 1976) in which first-order kinetics were found for CH_4 and half order for C_2H_4. These data can be rationalized by mechanisms that involve single-carbon atom species in rate limiting steps. The zero-order dependence on CH_4 at high concentrations may arise from adsorbed intermediates.

† 1 Torr ≈ 133 Pa.

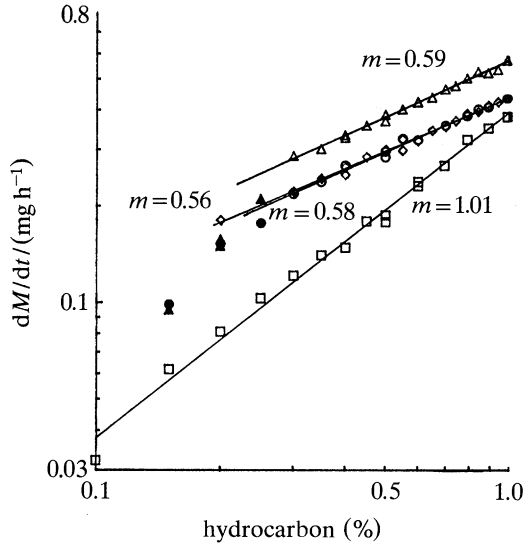

Figure 2. Log reaction rate against mole hydrocarbon (%) for various C_1 and C_2 gases. □, CH_4; ◇, C_2H_2; ○, C_2H_4; △, C_2H_6.

2. Diamond nucleation

The spontaneous nucleation of new diamond crystals under conditions where graphite is the stable carbon phase has been difficult to rationalize. Matsumoto & Matsui (1983) proposed, on the basis of symmetry arguments, that hydrocarbon cage compounds might serve as diamond precursors. It was proposed that a more likely precursor for diamond nucleation would be graphitic intermediates, which are subsequently hydrogenated by atomic hydrogen to saturated structures that can act as sites for diamond growth (Angus *et al.* 1988; Sunkara *et al.* 1990). Recent experimental studies support this latter view. Belton & Schmieg (1990) studied the nature of carbon bonding at different stages of nucleation on platinum substrates using X-ray photoelectron spectroscopy. They found that a carbon phase with graphitic bonding first formed, followed by a hydrogenated carbon phase and finally diamond. Microbalance studies of diamond nucleation and growth on platinum (Wang *et al.* 1992) show an initial induction period in which an oriented graphite deposit forms. Subsequently, this deposit disappears and the final deposit contains only polycrystalline diamond. A plot of the mass against time data and the observed Raman signals are shown in figure 3.

The nature of diamond nucleation can be probed by using graphite flakes as seed crystals. If the graphite is acting as a true nucleation site and not simply as an extra source of carbon, one would expect to find an orientational relation between the diamond and the original graphite substrate. Initial experiments on diamond growth on graphite seed crystals showed that the (111) diamond plane was parallel to the basal (0001) plane of the graphite (Angus *et al.* 1991). Subsequent experiments show that in addition to (111) diamond ‖ (0001) graphite, one often has a directional orientation within the planes, i.e. $[1\bar{1}0]$ diamond ‖ $[11\bar{2}0]$ graphite (Li *et al.* 1992). This relation means that the puckered six-membered rings in the diamond (111) planes retain the same orientation as the flat six-membered rings in the graphite basal (0001) plane. A transmission electron micrograph of one of these oriented

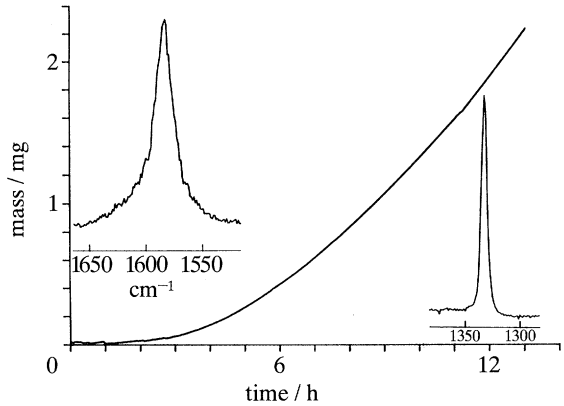

Figure 3. Mass of diamond against time in a microbalance hot-filament reactor. Inset at upper left shows Raman signal of graphite obtained during initial period (peak at 1581.8 cm^{-1}). Inset at lower right shows Raman signal of diamond obtained during steady state growth period (peak at 1333.1 cm^{-1}).

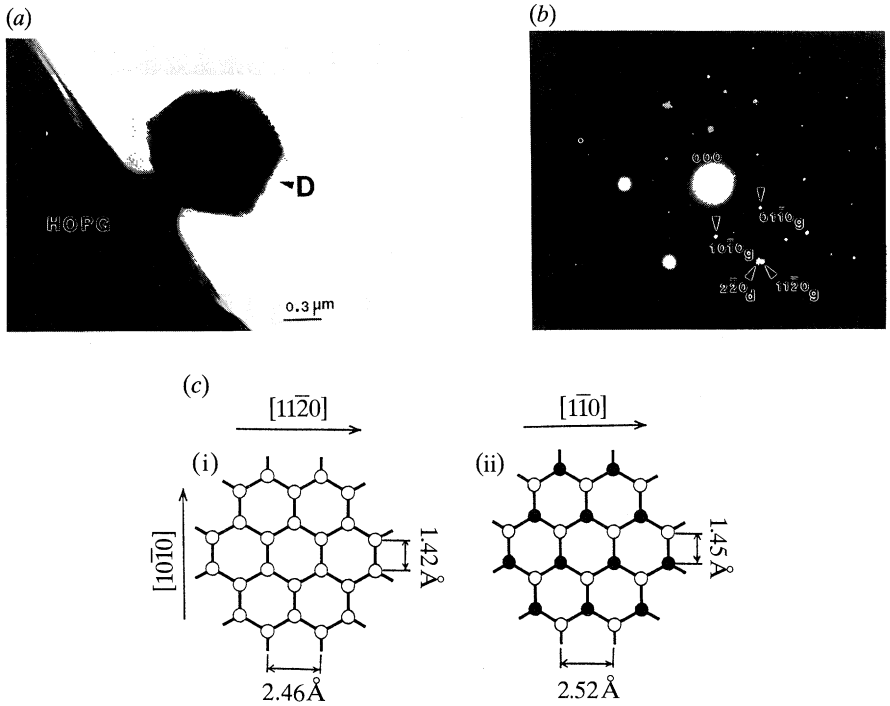

Figure 4. (*a*) Transmission electron micrograph of diamond nucleated on edge of highly oriented pyrolytic graphite. View is along normal to (0001) basal plane of graphite and the (111) plane of diamond. (*b*) Electron diffraction pattern from diamond and graphite shown in (*a*). (*c*) Orientation of (0001) graphite plane (i) and (111) diamond plane (ii).

diamond crystals on graphite, the corresponding diffraction pattern and the geometric relationship between the two structures are shown in figure 4.

The energetics of the conversion of graphitic, sp^2 bonded precursors can be examined by simple thermochemical calculations. Badziag *et al.* (1990) pointed out that hydrogen terminated 'diamonds' less than 3 nm in diameter have a lower

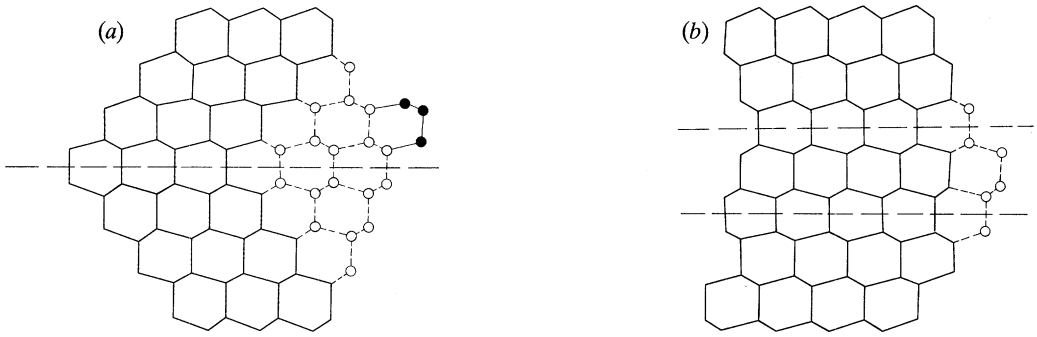

Figure 5. (*a*) ⟨110⟩ projection of diamond lattice containing one stacking error. Open circles and dashed lines show crystal filling out to smooth {111} surfaces with a convex corner. Three-atom nucleus shown on {111} surface with filled circles (permission *J. Mater. Res.*); (*b*) ⟨110⟩ projection of diamond lattice containing two stacking errors (extrinsic stacking fault). Open circles show crystal filling out to give a re-entrant (concave) corner. Two-atom nucleus shown with closed circles. Further growth can occur without the necessity of a three-atom nucleation event.

energy than hydrogen terminated graphite nuclei with the same number of carbon atoms. This means that in an environment rich in atomic hydrogen, the sp^3, tetrahedrally coordinated nuclei are in fact energetically favoured over the sp^2, trigonally coordinated nuclei. This work was subsequently criticized by Stein (1990), who pointed out that the correct parameter to consider is the free energy change for the appropriate reaction. However, Stein neglected to account for the fact that the active reagent under diamond growing conditions is atomic hydrogen, H, not molecular hydrogen, H_2. The enthalpy and free energy changes for the sequential hydrogenation of graphite to naphthalene and decalin by atomic hydrogen are:

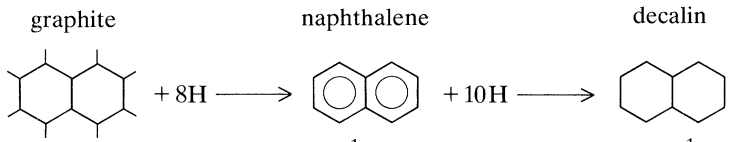

$\Delta G^\circ = -904.6$ kJ mol^{-1} $\quad$ $\Delta G^\circ = -1338.3$ kJ mol^{-1}

$\Delta G \leqslant -356.4$ kJ mol^{-1} $\quad$ $\Delta G \leqslant -653.1$ kJ mol^{-1}

(ΔG was calculated from nominal reaction conditions of 0.01 atomic fraction of hydrogen, pressure of 20 Torr and equal activities of naphthalene, decalin and graphite. Data were taken from Stull *et al.* (1969).) The estimated free energy changes at reaction conditions are strongly negative for these model reactions, which shows that graphitic nuclei can, indeed be converted into hydrogen saturated structures similar to diamond. Molecular orbital studies of the hydrogenation of single graphite sheets also support this conclusion (Angus *et al.* 1991; Mehandru *et al.* 1992). In addition, cyclopropane and cyclohexane are found as products when graphite is reacted with atomic hydrogen (Rye 1977). Other workers have also used thermodynamic methods to show that hydrogen stabilizes diamond surfaces (Sommer *et al.* 1989; Piekarcyk *et al.* 1989; Yarbrough *et al.* 1990; Harris *et al.* 1991).

The nucleation sequence may start with the formation of high molecular graphitic and polynuclear aromatic hydrocarbons (PAH) by the sequential polymerization of acetylene (Frenklach *et al.* 1985). These high molecular weight materials are sufficiently non-volatile so that they remain on the substrate until they become hydrogenated by atomic hydrogen, forming the saturated edge structure that is

PHILOSOPHICAL TRANSACTIONS OF THE ROYAL SOCIETY A MATHEMATICAL, PHYSICAL & ENGINEERING SCIENCES

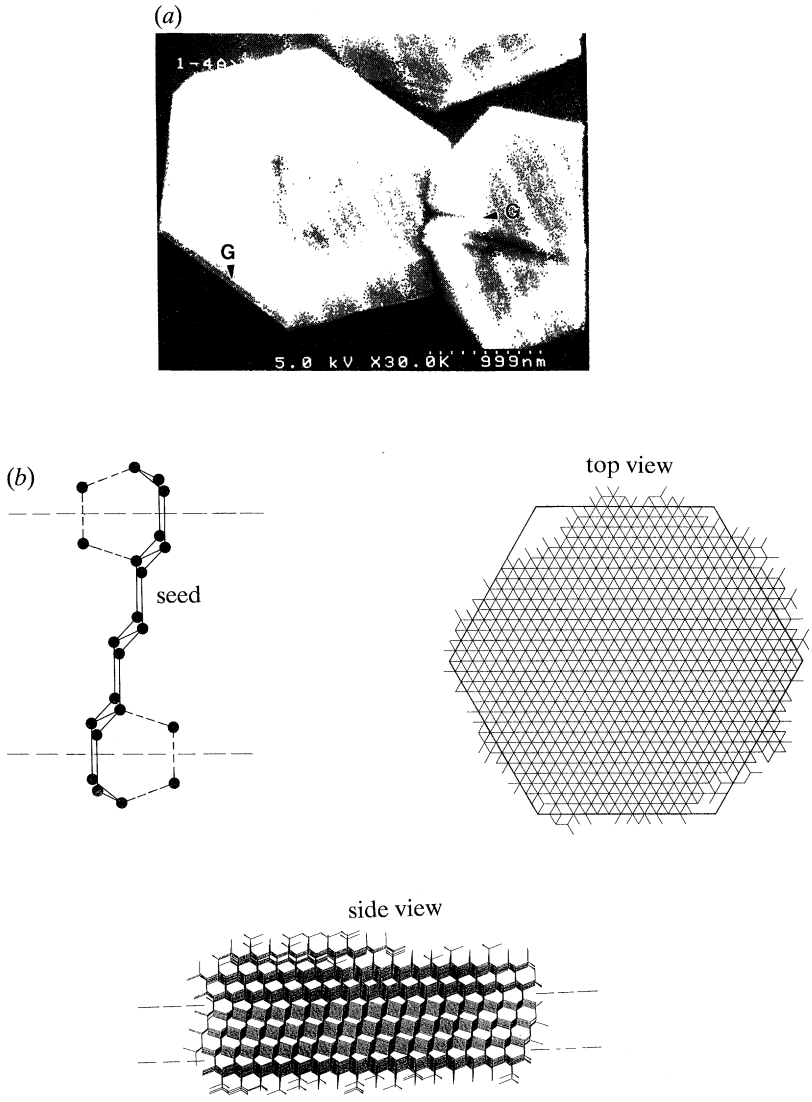

Figure 6. (*a*) Hexagonal diamond platelet and fully faceted three-dimensional diamond crystal. Re-entrant grooves are visible along the side faces of the hexagonal platelet and on the fully faceted crystal (marked with Gs). (*b*) Seed nucleus and top and side views of resulting hexagonal platelet grown by Monte Carlo simulation. Stacking errors are shown by dashed lines.

attractive for diamond nucleation. The atomic hydrogen plays a multiple role in this process. By terminating the dangling surface bonds it stabilizes the tetrahedrally coordinated, sp^3 nuclei with respect to the trigonally coordinated, sp^2 nuclei. It also serves as a reactive solvent which permits the conversion of graphitic nuclei into diamond nuclei, thereby circumventing the large activation barrier separating graphite from diamond. The mechanism is consistent with the careful observations of Lux, who showed that induction times for nucleation are shortest on those metals that can achieve a supersaturation of carbon on the surface the most rapidly (Joffreau *et al.* 1988; Lux & Haubner 1991).

Other methods of diamond nucleation are also possible. For example, growth

Table 2. *Relation of observed morphology to types of stacking errors during growth of* {111} *faceted crystals*

type of error	morphology
two stacking errors on parallel (111) planes (intrinsic or extrinsic stacking fault or micro twin)	hexagonal platelet
three stacking errors on parallel (111) planes	truncated hexagonal platelet
two stacking errors on non-parallel (111) planes	decahedral (pseudo five-fold symmetry)
three stacking errors on non-parallel (111) planes	icosahedral
single stacking error	triangular (macle)

on diamond debris left by scratching the substrate surface with diamond powder is commonly done (Iijima 1991).

The observed morphologies of vapour-grown diamond crystals range include: spherical clusters of diamond microcrystals, cubes, cubo-octahedrons, octahedrons and flat hexagonal platelets. Complex, multiply twinned forms (e.g. decahedrons and icosahedrons) are also observed. Twinned clusters, with many re-entrant surfaces, are perhaps the most common form, especially when in a regime that gives octahedral {111} faceting.

Defects that arise during growth can mediate further growth of the crystal. It appears that re-entrant corners play a major role in enhancing diamond growth rates. The re-entrants arise from the intersection of {111} twin bands or stacking faults with the surface. The re-entrant corners are favourable sites for nucleation of new layers. This effect has been known for many years in other contexts and was exploited for the rapid growth of silicon web from the melt. Presumably, the enhanced nucleation rate arises because only two atoms are required to form a stable nucleus at the re-entrant corner rather than three atoms that are required on a smooth {111} surface. This is shown schematically in figure 5. A recent discussion of the nucleation at re-entrant corners has been given by Tiller (1991).

Many complex morphologies can arise from the enhancement of growth rates by the re-entrant corners arising from multiple stacking errors (Sunkara 1992; Angus *et al.* 1991, 1992). A Monte Carlo computer program was used in which atoms were added to seed 'crystals' with different types of stacking errors (Sunkara 1992). A computer 'grown' hexagonal platelet and a scanning electron micrograph of a hexagonal diamond platelet are shown in figure 6. This morphology arises from the action of two parallel stacking errors. In the model shown in figure 6, the two stacking errors are separated by two layers of correct stacking. The growth rate within the plane of this microtwin is much greater than the growth rate normal to the plane because of the re-entrant corner on the periphery of the crystal. The result is a flat platelet of hexagonal shape and low aspect ratio. Hexagonal diamond platelets have been observed by several workers (Everson & Tamor 1991; Angus *et al.* 1991, 1992) and may reflect the nature of the precursor that leads to diamond nucleation. In a much earlier study, hexagonally shaped platelets of silver bromide were attributed to the mechanism described above (Berriman & Herz 1957).

Many other morphologies commonly observed in vapour-grown diamond can also be explained by the interaction of various combinations of stacking errors. These are summarized in table 2.

PHILOSOPHICAL TRANSACTIONS OF THE ROYAL SOCIETY A MATHEMATICAL, PHYSICAL & ENGINEERING SCIENCES

Table 3. *Comparison of mass and energy transport in diamond reactors*

type of reactor	Pe_{mass}	Pe_{thermal}
hot filaments	6×10^{-4}	8×10^{-4}
microwave	5×10^{-4}	7×10^{-3}
plasma torch	60	300
combustion	12	7

(Note that

$$Pe_{\text{mass}} = \frac{\langle u \rangle L}{D}\left[\frac{\text{mass flux by convection}}{\text{mass flux by diffusion}}\right],$$

$$Pe_{\text{thermal}} = \frac{\langle u \rangle L}{\alpha}\left[\frac{\text{thermal flux by convection}}{\text{thermal flux by diffusion}}\right],$$

where $\langle u \rangle$ is the average convective velocity, L is a characteristic length, D is the diffusion coefficient and α is the thermal diffusivity.)

4. Reactor environment

Much less attention has been paid to the transport processes within the reactor than to the attachment kinetics at the diamond surface. This is somewhat surprising since there is growing evidence that diamond growth rates may be limited by transport processes (Angus *et al.* 1989; Rau & Picht 1992). A complete understanding of diamond deposition must include a simultaneous solution of the energy and mass transport equations together with a detailed chemical mechanism. Simplified reactor models have been described (Debroy *et al.* 1990; Goodwin & Gavilett 1991; Kuczmarski *et al.* 1991). In the absence of a detailed reactor model, much of interest can be learned from an analysis of existing growth rate data.

A comparison of the transport of species and energy between the various types of reactors has been made (Angus *et al.* 1989, 1991). In the low pressure processes (e.g. microwave and hot-filament-assisted deposition) the transport is entirely dominated by molecular diffusion. Convection plays virtually no role. On the other hand, in the atmospheric pressure plasma torch and in atmospheric combustion, the transport is dominated by convection. An estimate of the magnitude of these effects can be obtained by computing average Peclet numbers. These results are shown in table 3. The growth rates in the atmospheric pressure, high gas velocity processes are much higher than in the low pressure processes. This is suggestive that the growth rate is limited by the rate of transport of species rather than by the attachment kinetics.

Similarly, the thermal Peclet numbers indicate that in typical hot-filament and microwave reactors, heat transport by conduction is much more important than heat transport by forced convection. The opposite is true in the plasma torch and combustion reactors.

The importance of natural convection in hot-filament reactors can be estimated from the Grashof number, Gr,

$$Gr = g\beta L^3 \Delta T/\nu^2, \tag{2}$$

where g is the acceleration of gravity, β the volumetric expansion coefficient, L a characteristic length, ΔT a temperature difference and ν the kinematic viscosity. The Grashof number is a measure of the relative magnitude of buoyancy forces to viscous

PHILOSOPHICAL TRANSACTIONS OF THE ROYAL SOCIETY A MATHEMATICAL, PHYSICAL & ENGINEERING SCIENCES

forces. For a hot-filament reactor containing primarily H_2 at 20 Torr, a ΔT of 1400 K and a characteristic (substrate to filament) length of 0.8 cm, we find $Gr \approx 0.7$, indicating that free convection is marginal at 20 Torr. This estimate indicates that in typical hot-filament reactors the flow is marginally stable to free convection and to roll cells. This conclusion is supported by direct measurements of heat transfer in a dual-filament diamond deposition reactor (Gat 1992; Gat & Angus 1992) and modelling studies (Kuczmarski *et al.* 1992; Kuczmarski 1992). The ability to use microbalances within the hot-filament reactor is further testimony to the unimportance of convection at these conditions.

Recent studies have shown that a significant amount of energy is transported by the decomposition of H_2 and subsequent recombination of H atoms (Yarbrough *et al.* 1992; Gat 1992; Gat & Angus 1992). Quantitative measurements of the energy released by the recombination of atomic H were made in a novel dual-filament reactor (Gat 1992). The power required to maintain a tungsten substrate wire at a fixed temperature was measured as a function of various process variables. By measuring the power to the substrate filament with an adjacent hot-filament on and off, the contribution of the atomic H recombination to the total energy transport could be quantitatively determined. The results show that in a typical hot-filament reactor, with the gas phase primarily hydrogen at 20 Torr, the energy transport by H atom recombination is approximately equal to that transferred by conduction. Furthermore, the contribution of convection is small at 20 Torr. The measurements of H atom recombination rate permits the determination of the net H atom diffusion flux from the hot-filament to the substrate. Under typical growth conditions there are approximately 10^4 H atom recombination events for each carbon atom added to the diamond. The large H atom recombination rate on the diamond surface leads to large gradients in H atom concentration in the gas phase. For one-dimensional transport between the hot-filament and the substrate the ratio of concentrations of atomic hydrogen, C_H, at the substrate and the hot-filament is given by

$$\frac{C_{H,s}}{C_{H,hf}} = \frac{1}{1+(2kT/\pi m)^{\frac{1}{2}}(\gamma l/D)}, \tag{3}$$

where D is the average diffusion coefficient of H, γ is the recombination coefficient, l is the filament to substrate distance, and m the mass of a hydrogen atom. For typical hot-filament conditions ($D = 0.175$ m^2 s^{-1}, $l = 0.01$ m, $T = 1000$ K and $\gamma = 0.5$), $C_{H,s}/C_{H,hf} \approx 0.1$. This is in general agreement with the results of Hsu (1991) and with recent reactor modelling studies in which the energy and species transport equations were solved for simple hot-filament geometries (Kuczmarski 1992). Despite the very large diffusion coefficient of H, the transport of H to the surface is partly diffusion limited.

5. Summary

A general understanding of the factors permitting diamond growth at low pressures has been achieved, although detailed molecular mechanisms are not known with certainty. Stacking errors formed during growth enhance growth rates and strongly influence the final crystal morphology. Nucleation of diamond can occur through graphitic intermediates or by growth on diamond debris left from scratching. In many processes the growth rates of diamond appear to be limited by transport processes rather than by attachment kinetics.

The support of a National Science Foundation Materials Research Group grant is gratefully acknowledged.

References

Angus, J. C., Will, H. A. & Stanko, W. S. 1968 Growth of diamond seed crystals by vapor deposition. *J. appl. Phys.* **39**, 2915–2922.

Angus, J. C., Gardner, N. C., Poferl, D. J., Chauhan, S. P., Dyble, T. J. & Sung, P. 1971 *Sin. Almazy* **3**, 38–40.

Angus, J. C., Hoffman, R. W. & Schmidt, P. H. 1988 Studies of amorphous hydrogenated diamondlike hydrocarbons and crystalline diamond. In *Science and technology of new diamond* (ed. S. Saito, O. Fukunaga & M. Yoshikawa), pp. 9–16. Tokyo: KTK/Terra.

Angus, J. C. 1989 History and current status of diamond growth at metastable conditions. In *Proc. First Int. Symp. on Diamond and Diamondlike Films*, pp. 1–13. Pennington, New Jersey: Electrochemical Society.

Angus, J. C., Buck, F. A., Sunkara, M., Groth, T. F., Hayman, C. C. & Gat, R. 1989 Diamond growth at low pressures. *MRS Bulletin* October, 38–47.

Angus, J. C., Li, Z., Sunkara, M., Gat, R., Anderson, A. B., Mehandru, S. P. & Geis, M. W. 1991*a* Nucleation and growth processes in chemical vapor deposition of diamonds. *Electrochem. Soc. Symp. Series*. Pennington, New Jersey: Electrochemical Society.

Angus, J. C., Wang, Y. & Sunkara, M. 1991*b* Metastable growth of diamond and diamondlike phases. *A. Rev. Mater. Sci.* **21**, 221–248.

Angus, J. C. 1991 Innovations in the chemical vapor deposition of diamond: perceptions of a participant. In *Japanese/American technological innovation* (ed. W. David Kingery), pp. 136–142. New York: Elsevier.

Angus, J. C., Sunkara, M., Sahaida, S. R. & Glass, J. T. 1992 Twinning and faceting in the early stages of diamond growth by chemical vapor deposition. *J. Mater. Res.* **7**, 3001–3009.

Badziag, P., Verwoerd, W. S., Ellis, W. P. & Greiner, N. R. 1990 Nanometre-sized diamonds are more stable than graphite. *Nature, Lond.* **343**, 244–245.

Badzian, A. R. & DeVries, R. C. 1988 Crystallization of diamond from the gas phase: part 1. *Mater. Res. Soc. Bull.* **23**, 385–400.

Belton, D. N. & Schmieg, S. J. 1990 States of surface carbon during diamond growth on Pt. *Surf. Sci.* **233**, 131–140.

Berman, R. & Simon, F. 1955 On the graphite-diamond equilibrium. *Z. Elektrochem.* **59**, 333–338.

Berriman, R. W. & Herz, R. H. 1957 Twinning and the tabular growth of silver bromide crystals. *Nature, Lond.* **180**, 293–294.

Bridgman, P. W. 1955 Synthetic diamonds. *Scient. Am.* **193**, 42–46.

Celii, F. G. & Butler, J. E. 1991 Diamond chemical vapor deposition. *A. Rev. Phys. Chem.* **42**, 643–684.

Chauhan, S. P., Angus, J. C. & Gardner, N. C. 1976 Kinetics of carbon deposition on diamond powder. *J. appl. Phys.* **47**, 4746–4754.

Chu, C. J., D'Evelyn, M. P. & Hauge, R. H. 1991 Mechanism of diamond growth by chemical vapour deposition on diamond (100), (111) & (110) surfaces: carbon-13 studies. *J. appl. Phys.* **70**, 1695–1705.

Davies, G. 1984 *Diamond*. Bristol: Adam Hilger Ltd.

Debroy, T., Tankala, K., Yarbrough, W. A. & Messier, R. 1990 Role of heat transfer and fluid flow in the chemical vapor deposition of diamond. *J. appl. Phys.* **68**, 2424–2432.

Deryagin, B. V., Spitsyn, B. V., Builov, L. L., Klochkov, A. A., Gurodetski, A. E. & Smolyaninov, A. V. 1976 Synthesis of diamond on non-diamond substrates. *Dokl. Akad. Nauk SSSR* **231**, 333–335.

Deryagin, B. V., Fedoseev, D. V., Spitsyn, B. V., Lukyanovich, D. V., Ryabov, B. V. & Lavrentev, A. V. 1968 Filamentary diamond crystals. *J. Cryst. Growth* **2**, 380–384.

DeVries, R. C. 1987 Synthesis of diamond under metastable conditions. *A. Rev. Mater. Sci.* **17**, 161–176.

Eversole, W. G. 1962 Synthesis of diamond. U.S. Patents 3,030,187 and 3,003,188.

PHILOSOPHICAL TRANSACTIONS OF THE ROYAL SOCIETY A MATHEMATICAL, PHYSICAL & ENGINEERING SCIENCES

Everson, M. P. & Tamor, M. A. 1991 Studies of nucleation and growth of boron-doped diamond microcrystals by scanning tunneling microscopy. *J. Vac. Sci. Technol.* B **9**, 1570–1576.

Frenklach, M. 1991 Molecular processes in diamond formation. In *Proc. Second Int. Symp. on Diamond Materials* (ed. A. J. Purdes, J. C. Angus, R. F. Davis, B. M. Meyerson, K. E. Spear & M. Yoder), vol. 91–98, pp. 145–153. Pennington, New Jersey: Electrochemical Society.

Frenklach, M., Clary, D. W., Gardiner, W. C. & Stein, S. E. 1985 Detailed kinetic modeling of soot formation in shock-tube pyrolysis acetylene. In *Proc. 20th Int. Symp. on Combustion*, pp. 887–901. Pittsburgh: The Combustion Institute.

Garrison, B. J., Dawnkaski, E. J., Srivastava, D. & Brenner, D. W. 1992 Molecular dynamics simulations of a dimer opening on a diamond (001) (2 × 1) surface. *Science, Wash.* **255**, 835–842.

Gat, R. 1992 Hot filament assisted deposition of diamond films. Ph.D. thesis, Case Western Reserve University, Cleveland, Ohio.

Gat, R. & Angus, J. C. 1992 Energy transport in hot-filament assisted deposition of diamond films. *J. appl. Phys.* (In the press.)

Goodwin, D. G. & Gavillet, G. G. 1991 Numerical modeling of filament-assisted diamond growth. In *Proc. 2nd Int. Conf. on New Diamond Science and Technology* (ed. R. Messier & J. T. Glass), pp. 335–340. Pittsburgh: Material Research Society.

Harris, S. J. & Wiener, A. M. 1985 Chemical kinetics of soot particle growth. *A. Rev. Phys. Chem.* **36**, 31–52.

Harris, S. J., Belton, D. N. & Blint, R. J. 1991 Thermochemistry on the hydrogenated diamond (111) surface. *J. appl. Phys.* **70**, 2654–2659.

Iijima, S., Aikawa, Y. & Baba, K. 1991 Growth of diamond particles in chemical vapor deposition. *J. Mater. Res.* **6**, 1491–1497.

Joffreau, P. O., Haubner, R. & Lux, B. 1988 Low pressure diamond growth on refractory metals. In *Proc. MRS Spring meeting*. Pittsburgh: Material Research Society.

Kamo, M., Sato, S., Matsumoto, S. & Setaka, N. 1983 Diamond synthesis from gas phase microwave plasma. *J. Cryst. Growth* **62**, 642–644.

Kuczmarski, M. A. 1992 Modelling of chemical vapor deposition reactors for silicon carbide and diamond growth. Ph.D. thesis, Case Western Reserve University, Cleveland, Ohio.

Kuczmarski, M. A., Washlock, P. A. & Angus, J. C. 1991 Computer simulation of a hot-filament CVD reactor for diamond deposition. In *Applications of diamond films and related materials* (Mater. Sci. Monographs) (ed. Y. Tzeng, M. Yoshikawa, M. Murakawa & A. Feldman), vol. 73, pp. 591–596. Amsterdam: Elsevier.

Lander, J. J. & Morrison, J. 1964 Low energy electron diffraction study of the (111) diamond surface. *Surf. Sci.* **2**, 241–246.

Leipunski, O. I. 1939 Synthetic diamonds. *Usp. Khim.* **8**, 1519–1534.

Li, Z., Wang, L., Suzuki, T., Argoitia, A., Pirouz, P. & Angus, J. 1992 Orientation relationship between chemical vapour deposited diamond and graphite substrates. *J. appl. Phys.* (In the press.)

Liander, H. & Lundblad, E. 1960 Some observations on the synthesis of diamonds. *Ark. Kemi.* **16**, 139–149.

Lux, B. & Haubner, R. 1991 Nucleation and growth of wear-resistant diamond coatings. In *Proc. Electrochemical Society Spring meeting*. Pennington, New Jersey: Electrochemical Society.

Matsui, Y., Matsumoto, S. & Setaka, N. 1983 TEM-electron energy loss spectroscope study of the diamond particles prepared by chemical vapor deposition from methane. *J. Mater. Sci. Lett.* **2**, 532–534.

Matsumoto, S., Sato, Y., Kamo, M. & Setaka, N. 1982*a* Vapor deposition of diamond particles from methane. *Jap. J. appl. Phys.* **2**, L183–L185.

Matsumoto, S., Sato, Y., Tsutsumi, M & Setaka, N. 1982*b* Growth of diamond particles from methane-hydrogen gas. *J. Mater. Sci.* **17**, 3106–3112.

Mehandru, S. P., Anderson, A. B. & Angus, J. C. 1992 Hydrogen binding and diffusion in diamond. *J. Mater. Res.* **7**, 689–695.

Piekarcyk, W., Roy, R. & Messier, R. 1989 Application of thermodynamics to the examination of the diamond CVD process from hydrocarbon-hydrogen. *J. Cryst. Growth* **98**, 765–776.

PHILOSOPHICAL TRANSACTIONS OF THE ROYAL SOCIETY A MATHEMATICAL, PHYSICAL & ENGINEERING SCIENCES

Rau, H. & Picht, F. 1992 Rate limitation in low pressure diamond growth. *J. Mater. Res.* **7**, 934–939.

Rossini, F. D. & Jessup, R. S. 1938 Heat and free energy of formation of carbon dioxide, and the transition between graphite and diamond. *J. Res. NBS* **21**, 491–513.

Rye, R. R. 1977 Reaction of thermal atomic hydrogen with carbon. *Surf. Sci.* **69**, 653–667.

Spitsyn, B. V. & Deryagin, B. V. 1956 Process for growing diamond grains. Author's patent certificate dated July 10, 1956; U.S.S.R. patent 339,134, May 5, 1980.

Stein, S. E. 1990 Diamond and graphite precursors. *Nature, Lond.* **346**, 517.

Sommer, M., Mui, K. & Smith, F. W. 1989 Thermodynamic analysis of the chemical vapor deposition of diamond films. *Solid State Commun.* **69**, 775–778.

Stull, D. R., Westrum, E. F. & Sinke, G. C. 1969 *The chemical thermodynamics of organic compounds*. New York: John Wiley.

Stull, D. R. & Prophet, H. 1971 *JANAF thermochemical tables*, 2nd edn. Washington, D.C.: National Bureau of Standards.

Sunkara, M. 1992 Monte Carlo simulation of diamond nucleation and growth. Ph.D. thesis, Case Western Reserve University, Cleveland, Ohio, U.S.A.

Sunkara, M., Angus, J. C., Hayman, C. C. & Buck, F. A. 1990 Nucleation of diamond crystals. *Carbon* **28**, 745–746.

Tiller, W. A. 1991 *The science of crystallization: microscopic interfacial phenomena*. New York: Cambridge University Press.

Wang, Y., Evans, E. & Angus, J. C. 1992 Diamond growth kinetics. *J. appl. Phys.* (Submitted.)

Yarbrough, W. A., Inspektor, A. & Messier, R. 1990 The chemical vapour deposition of diamond. In *Properties and characterization of amorphous carbon films* (ed. J. J. Pouch & S. A. Alterovich), pp. 151–174. Aedermannsdorf, Switzerland: Trans. Tech.

PHILOSOPHICAL TRANSACTIONS OF THE ROYAL SOCIETY A MATHEMATICAL, PHYSICAL & ENGINEERING SCIENCES

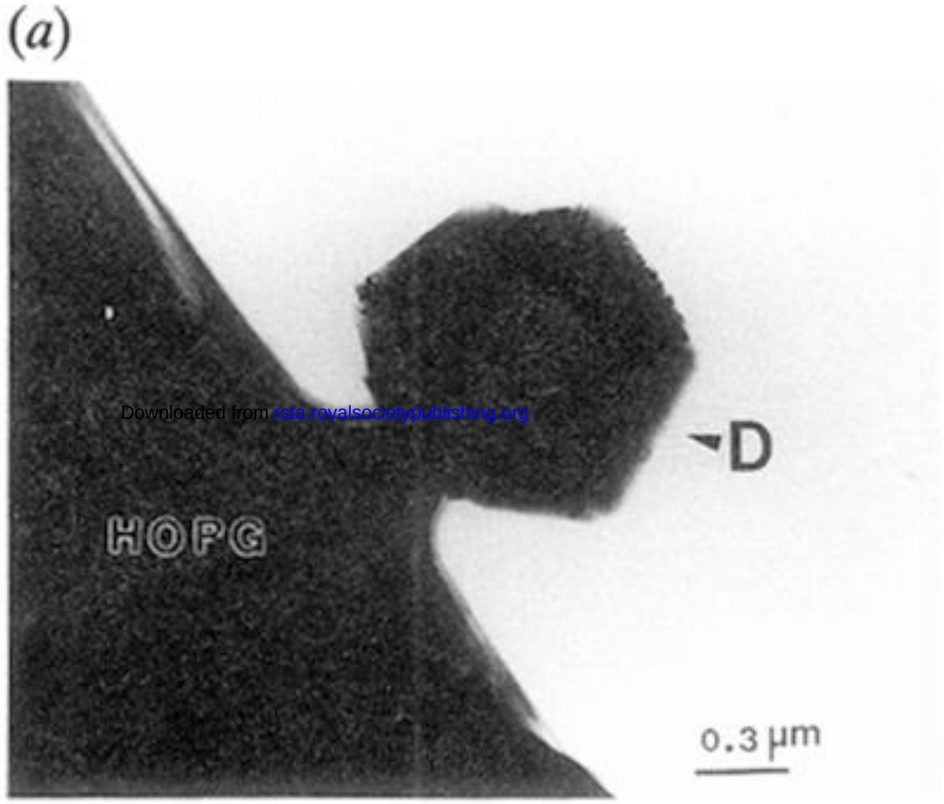

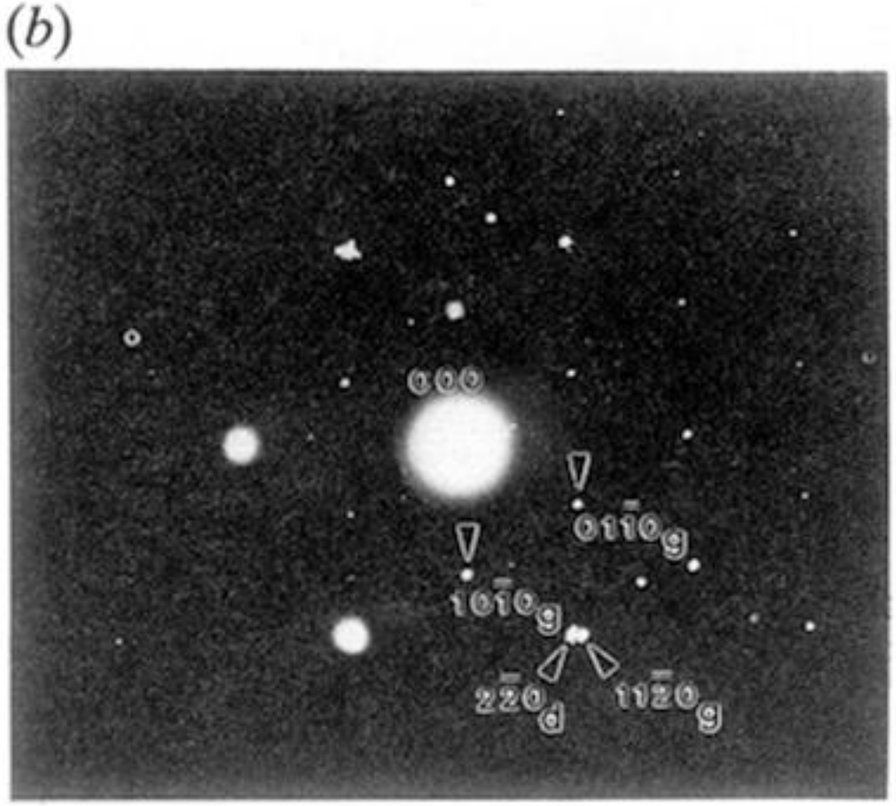

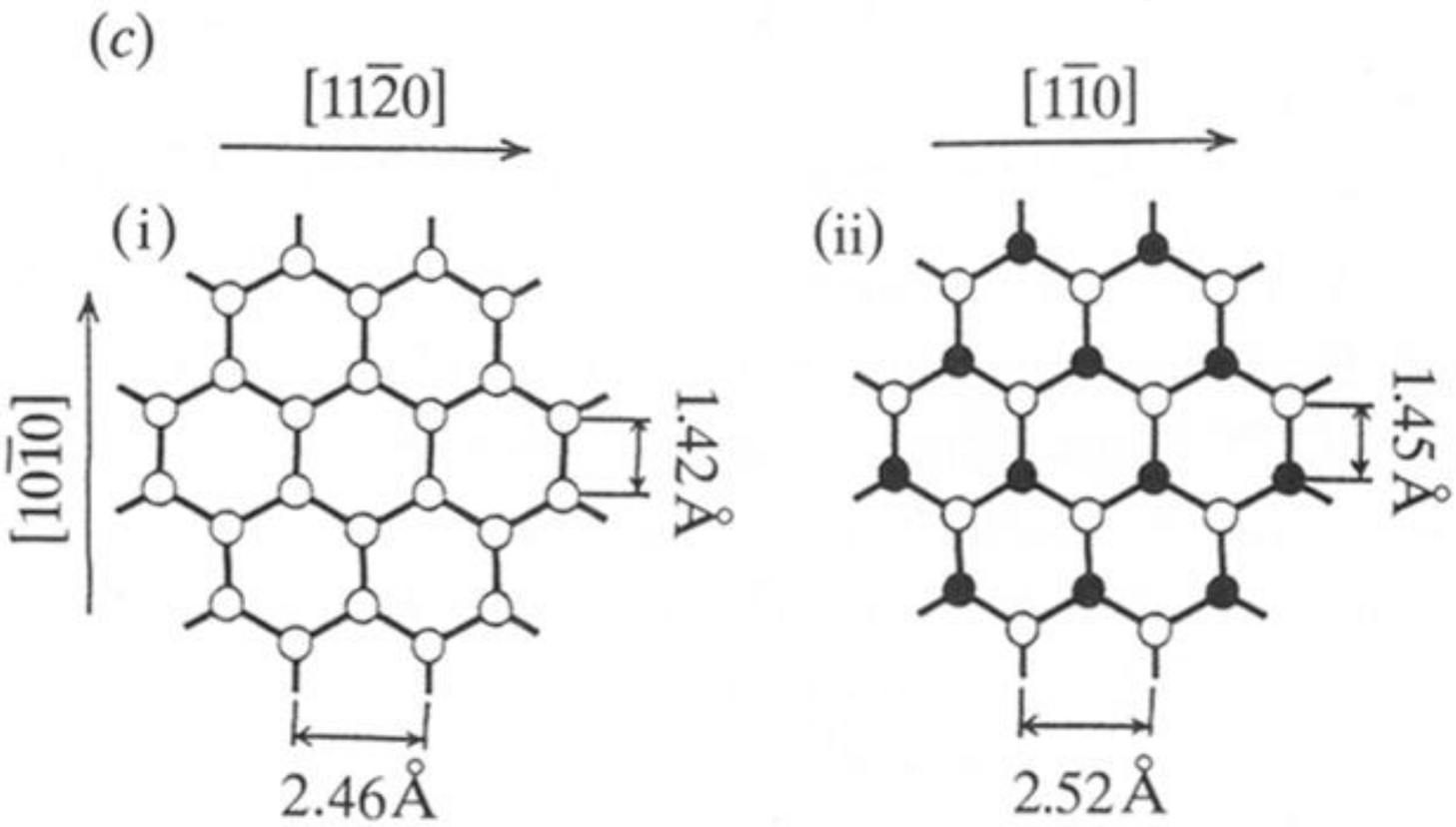

Figure 4. (*a*) Transmission electron micrograph of diamond nucleated on edge of highly oriented pyrolytic graphite. View is along normal to (0001) basal plane of graphite and the (111) plane of diamond. (*b*) Electron diffraction pattern from diamond and graphite shown in (*a*). (*c*) Orientation of (0001) graphite plane (i) and (111) diamond plane (ii).

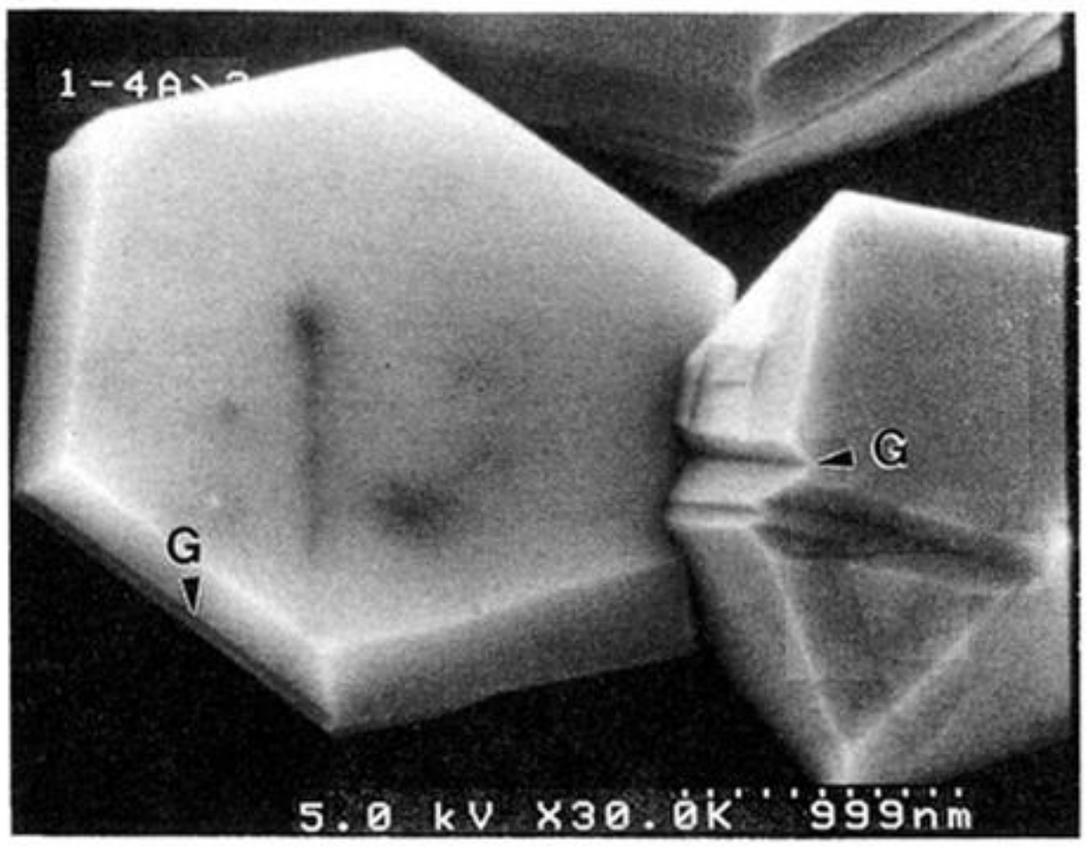

PHILOSOPHICAL TRANSACTIONS OF THE ROYAL SOCIETY A MATHEMATICAL, PHYSICAL & ENGINEERING SCIENCES

igure 6. (*a*) Hexagonal diamond platelet and fully faceted three-dimensional diamond crystal. Re-ntrant grooves are visible along the side faces of the hexagonal platelet and on the fully faceted rystal (marked with Gs). (*b*) Seed nucleus and top and side views of resulting hexagonal platelet rown by Monte Carlo simulation. Stacking errors are shown by dashed lines.